Sequence Specificity of DNA Cleavage by Bis(1,10-phenanthroline)copper(I): Effects of Single Base Pair Transitions on the Cleavage of Preferred Pyrimidine–Purine–Pyrimidine Triplets†

James M. Veal and Randolph L. Rill*

Department of Chemistry and Institute of Molecular Biophysics, The Florida State University, Tallahassee, Florida 32306-3006

Received August 31, 1988; Revised Manuscript Received December 7, 1988

ABSTRACT: The cleavage of DNA restriction fragments by bis(1,10-phenanthroline)copper(I) [$[(OP)_2Cu^I]^+$] is sequence dependent: the trimer TAT is most strongly preferred, while the trimer TGT and tetramers TAAT, TAGT, and CAGT are strongly to moderately preferred [Veal, J. M., & Rill, R. L. (1988) *Biochemistry 27*, 1822–1827]. $[(OP)_2Cu^I]^+$ cleavage of a series of oligonucleotide duplexes of the type 5′-CCCTPyPuPyCCCC-3′/3′-GGGAPuPyPuGGGG-5′ (Py = pyrimidine; Pu = purine) was examined to determine the effects of purine substituents in the central triplet on specificity. The relative cleavage rates of different PyPuPy triplets in oligomers were similar to those observed for restriction fragments. The undecamer duplex containing the trimer TAT (TTATC) was most preferentially cleaved, predominantly at the central adenosine and the adjacent 3′-thymidine. Duplexes differing from TTATC by a single A·T → G·C transition in the central triplet were cleaved at significantly reduced rates relative to TTATC, the order of preference being TAT > TGT > TAC > CAT. By contrast, duplexes differing from TTATC by a single A·T → I·C transition were cleaved at rates similar to those for TTATC when the transition occurred at the 5′-pyrimidine or central purine [i.e., C(·I)AT and TIT]. A duplex containing the trimer TAC(·I) was cleaved at a reduced rate similar to the duplex containing TAC(·G). The guanine 2-amino group at positions 1 and 2, but not position 3, of a 5′-PyPuPy-3′ trimer is therefore implicated as a strong inhibitor of DNA binding by the copper–phenanthroline complex. The influence of the guanine 2-amino group and other features of the cleavage at PyPuPy triplets can be rationalized by a partial intercalation binding model in which one phenanthroline ring system intercalates into the DNA minor groove at the 5′-PyPu-3′ step.

The complex bis(1,10-phenanthroline)copper(I) [$[(OP)_2Cu^I]^+$] binds noncovalently to double-stranded DNA and, in the presence of molecular oxygen and a reducing agent, produces hydroxyl radicals that cleave DNA strands in the region of binding [reviewed by Sigman (1986)]. $[(OP)_2Cu^I]^+$ has been used extensively as a "footprinting" reagent for determining ligand binding sites on DNA (Barton, 1986; Sigman, 1986). Minor groove binding of $[(OP)_2Cu^I]^+$ is evidenced by the ability of the complex to footprint netropsin, which binds in the minor groove, but not the restriction endonuclease *Eco*RI, which binds in the major groove (Kuwabara et al., 1986). Recently $[(OP)_2Cu^I]^+$ has also been used as a novel DNA sequence-specific cleaving agent when covalently coupled with oligonucleotides or sequence-specific DNA binding proteins (Chen & Sigman, 1986, 1987; Francois et al., 1988).

We have been interested in a different phenomenon—the relatively high sequence specificity of DNA cleavage by $[(OP)_2Cu^I]^+$ alone. Nonrandom cleavage of DNA was noted in earlier studies (Drew & Travers, 1984; Sigman, 1986; Suggs & Wagner, 1986; Flick et al., 1986). For example, strong recognition of the *lac* promotor Pribnow box and marked effects of point mutations within the Pribnow box on cleavage frequencies were observed by Spassky and Sigman (1985). Preferential cleavages of sequences 5′-flanking *Drosophila* heat shock and histone genes were also noted by Cartwright and Elgin (1982) and Jesse et al. (1982).

Recently we reported an analysis of $[(OP)_2Cu^I]^+$ cleavages on >2300 bases of DNA in restriction fragments, which indicated that sequence preferences of $[(OP)_2Cu^I]^+$ are determined primarily at the level of base triplets and quartets (Veal & Rill, 1988). The triplets TAT and TGT are strongly and moderately preferred, respectively, and the quartets TAAT, TAGT, TAGC, CAGT, and CAGC are also preferred. Predominant cleavage occurs at the A in TAT. In agreement with Drew and Travers (1984), we observed that polypyrimidine tracts are cleaved with low frequency, and cleavage on opposing complementary strands exhibits a 3′-stagger consistent with binding within the minor groove.

A comparison of the relative preferences of $[(OP)_2Cu^I]^+$ for pyrimidine–purine–pyrimidine triplets showed that cleavage frequencies are reduced for all permutations of TAT in which an A·T → G·C base pair transition occurs. An A·T → G·C transition maintains an exocyclic pyrimidine oxygen in the minor groove but replaces a minor groove proton by an amino group at the purine C2 position. Substitution of the bulky, partially charged, amino group into the minor groove may well inhibit binding, as is the case for the polypeptide antibiotics netropsin and distamycin (Kopka et al., 1985). This hypothesis can be tested by replacing G·C base pairs with I·C base pairs, inosine being identical with guanine except for a ($-NH_2 \rightarrow -H$) substitution at C2.

We have now examined the effects of such single base pair substitutions on the $[(OP)_2Cu^I]^+$ cleavage of pyrimidine–purine–pyrimidine sequences in DNA undecamer duplexes of the type 5′-CCCTPyPuPyCCCC/3′-GGGAPuPyPuGGGG. We observed that the TAT sequence was highly preferred but that A·T → G·C transitions reduce the reactivity of the central PyPuPy/PuPyPu triplet relative to TAT/ATA, as expected

†Supported by Grant ER60588 from the Department of Energy.

0006-2960/89/0428-3243$01.50/0

from studies on DNA restriction fragments. Substitution of inosine for guanine at either of the first two positions of a PyPuPy/PuPyPu triplet restored reactivity to a level comparable to that observed for TAT/ATA, while substitution at the third position had no effect. The cleavage pattern of the preferred tetramer TAGT was also examined in the undecamer CCCTTAGTCCC/GGGAATCAGGG.

Materials and Methods

$[(OP)_2Cu^I]^+$ Cleavage of a Restriction Fragment. Plasmid pUC18 was cleaved with the restriction endonuclease *Hin*fI; fragments were labeled on the 3′-end with [α-^{35}S]dATPαS by using AMV reverse transcriptase and then cleaved with restriction endonuclease *Hae*III. The 348 base pair fragment from the region between the ampicillin resistance gene and the origin was purified from a low melting point agarose gel after electrophoresis. The fragment was then reacted with $[(OP)_2Cu^I]^+$ as previously reported (Veal & Rill, 1988) and analyzed by densitometry as discussed below.

$[(OP)_2Cu^I]^+$ Cleavage of Undecamer Duplexes. Oligonucleotides were synthesized on an Applied Biosciences DNA synthesizer to prepare the following undecamer duplexes (hereafter abbreviated in the text as indicated in parentheses):

5′-CCCTTATCCCC	(TTATC)	CCCTTTTCCCC	(TTTTC)
3′-GGGAATAGGGG		GGGAACAGGGG	
5′-CCCTTGTCCCC	(TTGTC)	CCCTTAGTCCC	(TTAGT)
3′-GGGAACAGGGG		GGGAATCAGGG	
5′-CCCTTACCCCC	(TTACC/I)	CCCTCATCCCC	(TCATC/I)
3′-GGGAATIGGGG		GGGAITAGGGG	
CCCTCATCCCC	(TCATC/G)	CCCTTACCCCC	(TTACC/G)
GGGAGTAGGGG		GGGAATGGGGG	

Protective groups were removed by overnight incubation in ammonia at 55 °C. After evaporation of the ammonia the oligonucleotides were resuspended in kinase buffer and labeled on the 5′-end with [γ-^{35}S]dATPγS by using T4 polynucleotide kinase. Labeled oligonucleotides were purified by electrophoresis on 20% denaturing polyacrylamide gels and extraction by overnight incubation at 37 °C in 1 mL of 500 mM ammonium acetate/10 mM EDTA. Eluted oligonucleotides were desalted with Sep-Pak C-18 reverse-phase columns. The purified oligonucleotides were annealed to their complementary strand by mixing, heating at 90 °C for 5 min in buffer, and allowing to air cool to room temperature.

$[(OP)_2Cu^I]^+$ reactions were typically carried out with 50 μM 1,10-phenanthroline, 10 μM Cu, 100 mM Tris·HCl, pH 8.0, 4 mM mercaptopropionic acid, and 0.1–0.2 nmol of DNA. Reactions were initiated by addition of the mercaptopropionic acid. At appropriate time intervals (2–64 min), aliquots were removed from the reaction mix and the cleavage reaction was quenched by addition of neocuproine. Sample preparation for electrophoresis was complicated by the fact that ethanol precipitation caused differential precipitation of DNA fragments according to size. Moreover, in our hands, differential loss of short products occurred when C-18 reverse-phase columns were used. Consequently, it was necessary to dry all reaction mixes in vacuo. Low initial reaction volumes were used to keep final salt concentrations reasonable and minimize salt gradients during electrophoresis. After two extractions with H_2O-saturated butanol the aliquots were dried in vacuo and resuspended in a buffer containing 9 mM boric acid, 0.25 mM EDTA, 0.025% xylene cyanol FF, and 5 mM dithiothreitol. DTT was included because in its absence two primary parent bands were repeatedly observed. The slower moving band was eliminated by addition of the DTT, which may scavenge metals interacting with the incorporated ^{35}S. EDTA also eliminated the secondary band, but high EDTA concentrations caused severe salt gradients. The samples were electrophoresed on 20% denaturing polyacrylamide gels for 2–3 h at 2000 V/25 mA. The gels were then covered with cling wrap and autoradiographed undried at −80 °C for varying exposure times.

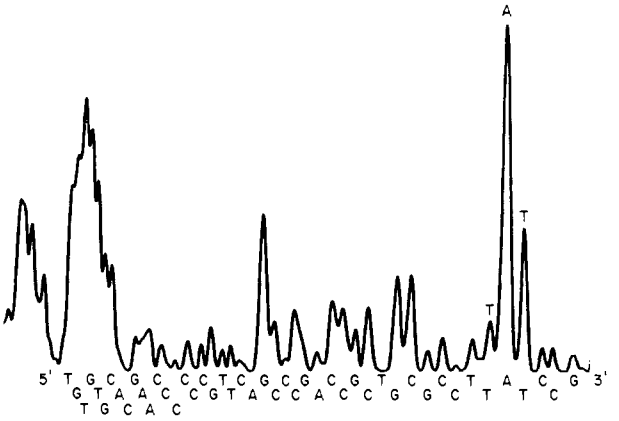

FIGURE 1: Cleavage pattern of a DNA *Hin*fI/*Hae*III restriction fragment of pUC18 reacted with $[(OP)_2Cu^I]^+$. Positions of cleavage were determined by comparison to an adenine + guanine sequencing reaction. The sequence CCTTATCC occurs 23 base pairs from the labeled *Hin*fI end. Note the strong cleavage of the adenosine of the TAT step, the lesser cleavage of the adjacent 3′-thymidine, and the low cleavage of the flanking pyrimidine tracts.

Densitometry. Densitometry of autoradiograms was performed with a Bio-Rad Model 620 videodensitometer interfaced to Bio-Rad Model 3392A integrator. Restriction fragment products were identified by comparison with A+G sequencing reactions. No external size markers were required for the oligonucleotide reactions because, in all gels, products of two or more oligonucleotides differing in sequence by a single base (hence differing in mobility) were electrophoresed simultaneously, thereby providing an internal size marker. Intensities of bands from different oligonucleotides were normalized by the combined intensities of the cytosines at positions 9 and 10 of each duplex (see Table I). Since only a small fraction of the parent oligonucleotides was degraded in each case, the relative band intensities reflect the relative rates of cleavage at each site.

Results

Cleavage of a Restriction Fragment Containing the Highly Preferred CCTTATCC Sequence. The sequence CCTTATCC/GGATAAGG occurs approximately 26 base pairs from the labeled *Hin*fI end of the 348 base pair *Hin*fI/*Hae*III fragment of pUC18 (Figure 1). The distribution of cleavage intensities within this sequence was characteristic of a PyTATPy sequence (Veal & Rill, 1988) and illustrates the strong preference for adenosine in these sequences. As observed for all TAT sequences, cleavage at the thymidine 3′-flanking the preferred adenosine was greater than cleavage at the 5′-flanking thymidine. That the TAT sequence alone was responsible for the high cleavage was demonstrated by the uniformly low cleavage of the sequence CCTTTCTCCCTTC located 153 base pairs from the *Hin*fI end (data not shown).

Cleavage of the TTATC Undecamer Duplex. The oligonucleotide TTATC contains the highly preferred TAT triplet flanked by disfavored pyrimidine tracts. While $[(OP)_2Cu^I]^+$ cleaves all base sequences to some degree, this juxtaposition

Table I: Relative Extents of Cleavage at Specific Sites in Oligonucleotide Duplexes

	band intensity of indicated base[b]							
duplex[a]	C	T	T(C)	A(I,G)	T(C)	C	C	C
TTATC	1.3	2.2	4.6	20.7	15.0	4.9	1.8	1.0
	(100)	(100)	(100)	(100)	(100)	(100)	(100)	(100)
TCATC/I	1.1	1.8	3.8	19.1	12.2	4.5	1.7	1.1
	(83)	(82)	(83)	(93)	(81)	(93)	(96)	(107)
TCATC/G	0.6	0.9	1.7	1.4	1.6	1.3	1.9	0.9
	(46)	(41)	(38)	(7)	(10)	(27)	(104)	(93)
TTITC	1.0	2.8	5.2	20.2	14.6	4.4	1.8	1.0
	(77)	(129)	(114)	(98)	(97)	(90)	(98)	(103)
TTGTC	0.8	1.7	1.9	11.6	12.7	3.4	1.8	1.0
	(57)	(78)	(42)	(56)	(84)	(71)	(99)	(102)
TTACC/I	0.5	1.0	1.3	4.6	3.6	1.8	1.8	1.0
	(36)	(44)	(28)	(22)	(24)	(38)	(98)	(103)
TTACC/G	1.0	1.6	2.7	7.6	6.2	3.6	1.7	1.1
	(73)	(73)	(60)	(37)	(42)	(75)	(96)	(108)
	band intensity of indicated base[b]							
duplex[a]	C	T	T	A	G	T	C	C
TTAGT	0.5	1.3	3.1	10.3	12.6	11.8	1.9	0.9
	(38)	(57)	(68)	(50)	(84)	(243)	(104)	(93)

[a] Duplexes are abbreviated as indicated under Materials and Methods. [b] Oligonucleotides containing the central PyPuPy sequence were labeled on the 5′-end with [^{35}S]thiophosphate, annealed to the unlabeled complementary strand, and then reacted slightly with $[(OP)_2Cu^I]^+$. Products were electrophoresed on 20% polyacrylamide gels. Autoradiograms were quantitated by densitometry. Band intensities were normalized relative to the combined intensities for bands corresponding to products of cleavage at C9 and C10 of each duplex. The numbers in parentheses indicate the percent of cleavage of a given base compared to cleavage at the base in the equivalent position in the duplex TTATC.

of highly preferred and disfavored sequences creates an oligonucleotide that should have a unique, central, strong binding site. The elimination of multiple equivalent binding sites, in conjunction with the use of high-resolution 20% acrylamide gels and the weakly β-emitting ^{35}S isotope, permitted a detailed analysis of cleavage products and the effects of single base pair transitions. The pattern of $[(OP)_2Cu^I]^+$ cleavage of the *Hin*fI/*Hae*III restriction fragment provides a reference for studies of the undecamer duplexes. The electrophoretic pattern of oligonucleotide products (Figure 2) is more complicated, however, because multiple products of attack at a single nucleotide are resolved on 20% polyacrylamide gels (Kuwabara et al., 1986; see also below). These were summed to calculate the cleavage frequency at each nucleotide (Table I).

$[(OP)_2Cu^I]^+$ attack on TTATC was analogous to that of the restriction fragment in that the central adenosine was most reactive and the 3′-thymidine was more reactive than the 5′-thymidine (Figure 2). Both nearest-neighbor thymidines were cleaved more frequently than flanking sequences. Some differences were observed in the relative frequencies of products of individual bases. Most apparent was the difference in the ratio of products from the central adenosine and 3′-thymidine. This ratio was approximately 3:1 for AT in the restriction fragment but only 1.4:1 for the oligonucleotide duplex. Moreover, C8 of TTATC was cleaved more intensely than the corresponding cytidine of the restriction fragment. The overall specificities of cleavage of the TAT sequence relative to flanking cytidines were similar, however. For example, the ratio of the sum of cleavage frequencies at all positions of TAT of the restriction fragment to the intensity of cleavage at the 3′-flanking cytidine was 36:1; for the TTATC duplex this ratio was 25:1.

Specific Products of the Cleavage of TTATC. As first noted by Kuwabara et al. (1986), three types of products can result from $[(OP)_2Cu^I]^+$ attack of a given nucleotide (Figure 3). The predominant product results from proton abstraction at C1′ and is a 3′-phosphomonoester—the product of a Maxam–Gilbert chemical sequencing reaction. An unstable, slower migrating, product was shown by Goyne and Sigman (1987) to be a 3′-phospho-5-methylfuranone (3′-PMF) intermediate from proton abstraction at C1′. The fastest migrating product is a 3′-phosphoglycolate, also noted upon ^{60}Co irradiation of DNA (Henner et al., 1982, 1983), resulting from proton abstraction at C4′.

Table II: Specific Cleavage Products from Positions 6 and 7 of the Duplexes TTATC, TTGTC, TTITC, TTACC/G, and TTACC/I

duplex[a]	intensities (%) of cleavage products of indicated base[b]	
	A6	T7
TTATC	1.8 (9)/13.1 (63)/5.8 (28)	4.0 (27)/9.2 (61)/1.8 (12)
	I6	T7
TTITC	2.9 (14)/11.4 (56)/6.0 (30)	5.0 (34)/7.9 (54)/1.8 (12)
	G6	T7
TTGTC	2.6 (23)/6.7 (57)/2.4 (20)	2.3 (18)/7.9 (62)/2.5 (20)
	A6	C7
TTACC/I	0.3 (7)/3.5 (73)/1.0 (20)	0.8 (20)/3.1 (80)/0.0 (0)
TTACC/G	0.9 (12)/5.1 (67)/1.6 (21)	1.2 (20)/5.1 (80)/0.0 (0)

[a] Duplex abbreviations are given under Materials and Methods. [b] The normalized intensities of cleavage products for a given base (in the order 3′-phosphoglycolate/3′-phosphomonoester/furanone intermediate) are shown opposite the percentage composition of cleavage products at that base (in parentheses). The 3′-phosphoglycolate is derived from proton abstraction at the deoxyribose C4′, while the 3′-phosphomonoester and furanone intermediates are derived from proton abstraction at the deoxyribose C1′. See Materials and Methods and footnote *b* in Table I for procedures.

Significant amounts of all three products were obtained from the oligomer TTATC when samples were electrophoresed immediately after $[(OP)_2Cu^I]^+$ reaction (Figure 2a). Although the 3′-phosphomonoester product of C1′ attack predominanted in all cases, the relative amounts of the three products varied strikingly for individual nucleotides, in particular for the adenosine and 3′-flanking thymidine (Table II). Attack of the central adenosine yielded a significant percentage of the 3′-phospho-5-methylfuranone product, but a relatively small amount of 3′-phosphoglycolate—28% and 9% of the total products, respectively. By contrast, the 3′-thymidine yielded 27% 3′-phosphoglycolate and only 12% 3′-phospho-5-

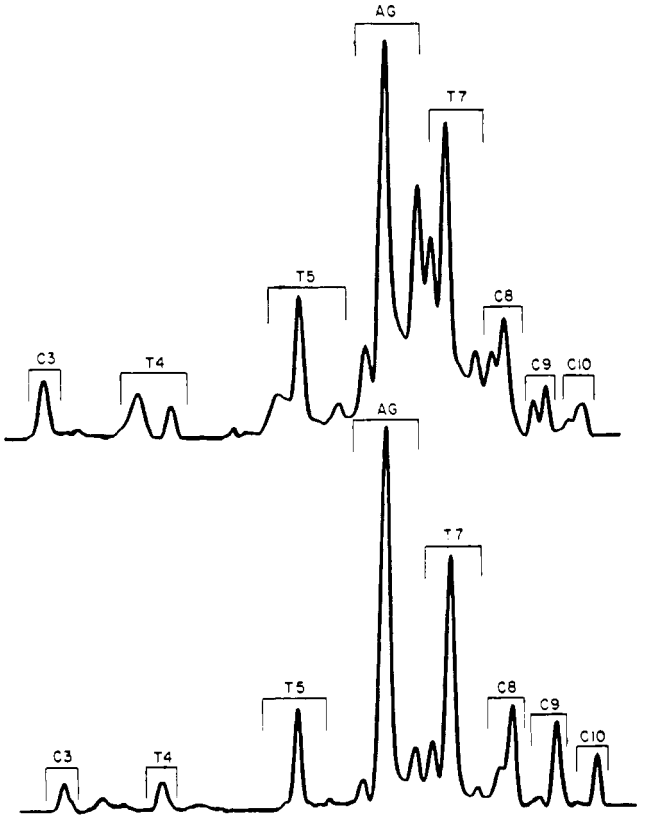

FIGURE 2: Cleavage pattern of the oligonucleotide duplex TTATC reacted with $[(OP)_2Cu^I]^+$. Reaction conditions were identical in the upper and lower frames except that the duplex in the upper frame was reacted with $[(OP)_2Cu^I]^+$ and products were immediately loaded on a polyacrylamide gel, whereas for the lower frame products were stored at −80 °C for 48 h prior to electrophoresis. Multiple products of cleavage at a single base are bracketed and occur in the order 3′-phosphoglycolate, 3′-phosphomonoester, and unstable 3′-phospho-5-methylfuranone. The latter two products are derived from proton abstraction at C1′, while the 3′-phosphoglycolate is derived from proton abstraction at C4′ (see Figure 3 and text for discussion). The 3′-phosphomonoester was the primary cleavage product at all bases.

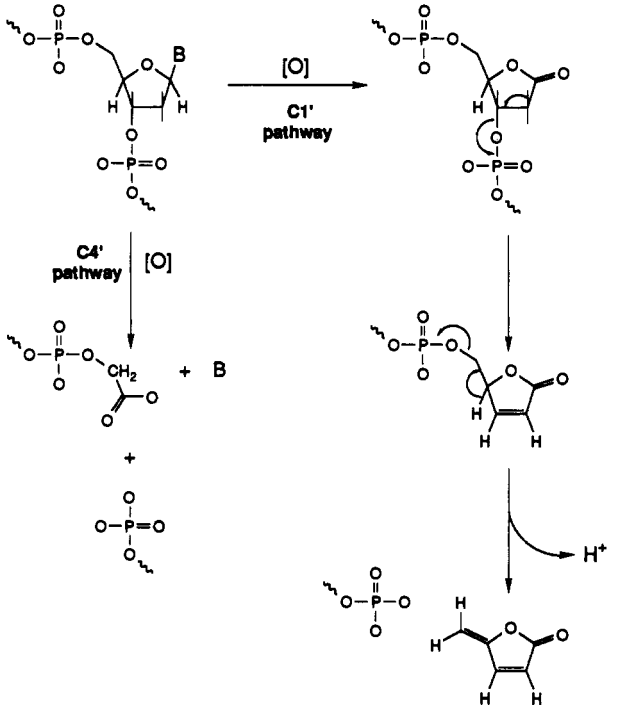

FIGURE 3: Reaction pathways for DNA chain cleavage caused by hydroxyl radical abstraction of a proton at deoxyribose C1′ or C4′. Proton abstraction from C4′ yields a 3′-phosphoglycolate, whereas proton abstraction from C1′ produces an unstable 3′-phospho-5-methylfuranone that decomposes to yield a 3′-phosphomonoester. Figure adapted from Goyne and Sigman (1987).

methylfuranone, while the cytidine 3′-flanking the TAT trimer yielded almost equal amounts of 3′-phosphoglycolate and 3′-phosphomonoester (44% and 55%, respectively; data not shown) but no detectable furanone. Both the 3′-phosphoglycolate and proposed 3′-phospho-5-methylfuranone products were unstable, especially the latter. When stored for greater than 48 h in sample buffer, they degraded to the corresponding 3′-phosphomonoester (Figure 2).

Effects of Single Base Pair Transitions. The effects of single A·T → G·C or I·C transitions on the sensitivities of PyPuPy sequences to $[(OP)_2Cu^I]^+$ cleavage were examined directly by comparing reactions of undecamer duplexes that were permutations of TTATC with a single G·C or I·C substitution within the central TAT trimer. The terminal cytidines of these oligonucleotide duplexes are expected to be sufficiently distant from the central trimer to be unaffected by the substitutions; thus the intensities of bands corresponding to cleavage at C9 and C10 were used as internal standards to normalize band intensities obtained from different duplexes.

Comparison of the cleavages of TTATC and TCATC/G showed that an A·T → G·C transition at position 5 caused total loss of preference by $[(OP)_2Cu^I]^+$ (Figure 4 and Table I). Cleavages at the central adenosine and 3′-thymidine of TCATC/G were reduced an order of magnitude relative to TTATC, to a level comparable to that of the terminal cytidines. By contrast, replacing the A·T base pair at position 5 of TTATC with an I·C base pair (TCATC/I) caused only a 10% reduction in cleavage at the central PyPuPy triplet relative to TTATC (Figure 4 and Table I).

Similar results were obtained for an A·T → G·C or I·C transition at position 6, as determined by a comparison of reactions with TTGTC and TTITC (Figure 5). The guanosine and 3′-flanking thymidine were preferred relative to the flanking cytidines (Table I), but reactivities were reduced relative to TTATC, particularly at the guanosine, which was cleaved at approximately half the frequency of the adenosine of TTATC. Cleavage was observed to be almost evenly distributed between the guanosine and thymidine, with a slight preference to the thymidine. As with TCATC/I, substitution of an I·C base pair at position 6 (TTITC) maintained the preferred reactivity observed for TTATC (Figure 5 and Table I).

The final base pair substitutions examined were those at position 7. Consistent with the other A·T → G·C transitions, substitution of a G·C base pair at position 7 (TTACC/G) caused a reduction in $[(OP)_2Cu^I]^+$ cleavage at the central PyPuPy sequence relative to TTATC (Figure 5 and Table I). Cleavages of the adenosine and 3′-flanking cytidine in TTACC/G were nearly equal, with the adenosine slightly preferred. The reduction in relative frequency of cleavage at the central PyPuPy sequence in TTACC/G was less than observed for TCATC/G, but greater than observed for TTGTC. These results agreed with the hierarchial preferences seen for $[(OP)_2Cu^I]^+$ cleavage of PyPuPy triplets in restriction fragments (Veal & Rill, 1988). The effect of an I·C substitution at position 7 is shown by the cleavage pattern of TTACC/I (Figure 5). By contrast to the two other undecamer duplexes containing I·C substitutions, the preference for cleavage at the central PyPuPy triplet clearly was not restored to a level comparable with that of TTATC, but was

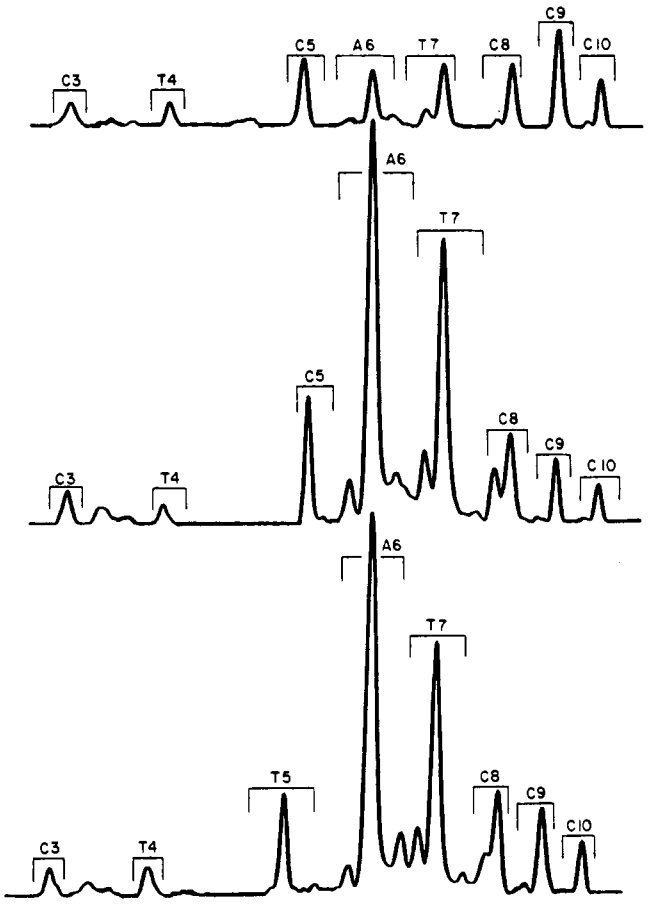

FIGURE 4: Comparison of the cleavage patterns of the oligonucleotide duplexes TCATC/G, TCATC/I, and TTATC (tracings, top to bottom) reacted with $[(OP)_2Cu^I]^+$. Products were allowed to stand for 48 h in sample buffer prior to electrophoresis. Note that the T → C transition alters the mobilities of the fragments that contain the transition and thereby provides an internal marker for identification of the cleavage products.

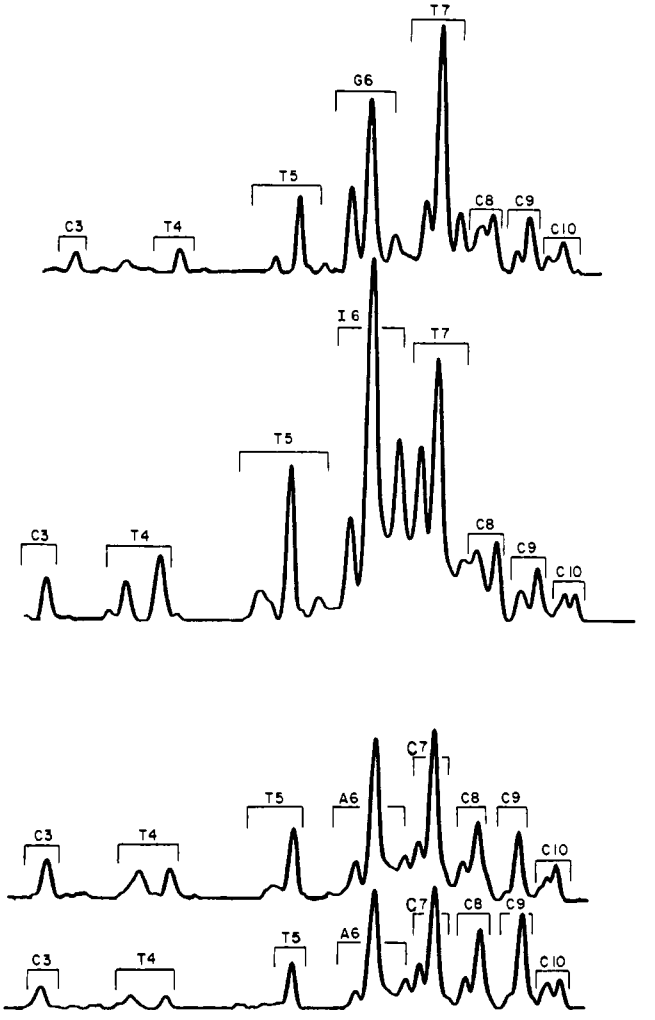

FIGURE 5: Comparison of the cleavage patterns of the oligonucleotide duplexes TTGTC, TTITC, TTACC/G, and TTACC/I (top to bottom) reacted with $[(OP)_2Cu^I]^+$. Products were electrophoresed immediately following the cleavage reaction, allowing detection of unstable intermediates.

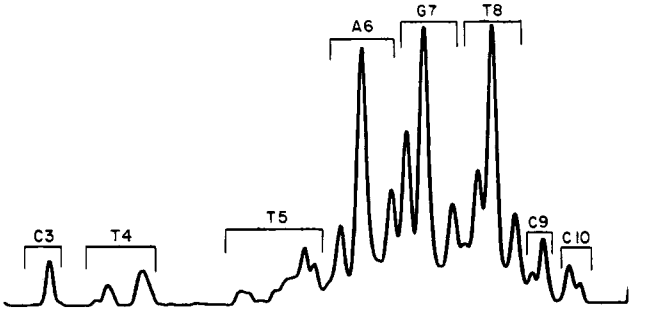

FIGURE 6: Cleavage pattern of the oligonucleotide duplex TTAGT reacted with $[(OP)_2Cu^I]^+$. Products were electrophoresed immediately following the cleavage reaction, allowing detection of intermediates.

actually reduced relative to TTACC/G.

Levels of Individual Base Products. Base pair substitutions affected the ratios of specific products of individual nucleotides, as well as the relative rates of nucleotide cleavage. Table II summarizes the products of the central purine and 3′-flanking pyrimidine (positions 6 and 7) of the TTATC, TTGTC, TTITC, TTACC/G, and TTACC/I duplexes. In each case the 3′-phosphomonoester predominanted, but significant amounts of 3′-phosphoglycolate and 3′-phospho-5-methylfuranone were observed, and the relative yields of the three products varied between duplexes. With the exception of TTGTC, the amount of the 3′-phospho-5-methylfuranone product of cleavage at position 6 exceeded the amount of the 3′-phosphoglycolate product, whereas for cleavage at position 7 the opposite was true. The duplex TTGTC yielded nearly equal amounts of both products at each position.

Although the overall cleavage of the guanosine at position 6 of TTGTC was significantly reduced relative to the adenosine of TTATC, the relative amount of 3′-phosphoglycolate product actually increased. This increase, approximately 50%, was also mainfested by the inosine of TTITC. Conversely, TTGTC showed reduced levels of 3′-phosphomonoester and 3′-phospho-5-methylfuranone products, relative to TTATC, which more than compensated for the increased 3′-phosphoglycolate levels. Cleavage of TTITC produced slightly less 3′-phosphomonoester than TTATC. TTACC/G and TTACC/I yielded reduced levels of all three products, relative to TTATC, and the ratios of products were approximately equivalent to TTATC. The most pronounced difference noted in products of cleavage at position 7 was that the cytidines of TTACC/G and TTACC/I yielded negligible 3′-phospho-5-methylfuranone, while the thymidines of TTATC, TTGTC, and TTITC yielded significant furanone.

Cleavage of TTAGT. The central TAGT quartet of the TTAGT duplex was preferentially cleaved by $[(OP)_2Cu^I]^+$ (Figure 6), as expected from previous studies of restriction fragments (Veal & Rill, 1988). Significant cleavage occurred

at positions 6, 7, and 8, with the guanosine preferred slightly over the flanking adenosine and thymidine. TTAGT was, thus, distinct from TTATC and other preferred PyPuPy sequences in that there were three strongly preferred sites of cleavage for TTAGT but only two for TTATC. Moreover, the most preferred base was the guanosine of TTAGT vs the adenosine of TTATC, reflecting an overall 3′-shift relative to the TA step. Although the overall intensities of cleavage of the adenosine, guanosine, and 3′-thymidine were similar, the ratios of the specific products differed significantly. As with the other duplexes, the 3′-phosphomonoester was the primary product (A, 59%; G, 52%; T, 55%). Cleavage of the adenosine produced more 3′-phospho-5-methylfuranone (24%) than 3′-phosphoglycolate (17%), while both the guanosine and adjacent thymidine produced more 3′-phosphoglycolate than furanone (29%–19% for the G, 30%–16% for the T).

Discussion

These data support and extend previous inferences about the sequence specificity of $[(OP)_2Cu^I]^+$ cleavage of DNA. The $[(OP)_2Cu^I]^+$ complex is unique in that it shows significant sequence preferences while lacking substituents capable of hydrogen bonding. An understanding of the structural features determining this specificity may provide insights into properties of DNA that govern ligand binding, independent of hydrogen-bond formation.

Elucidation of the mechanism of binding of $[(OP)_2Cu^I]^+$ to preferred DNA sites by NMR or X-ray crystallographic means requires use of short oligonucleotides containing a single strong binding site. Inherent in such studies is the assumption that the conformation and binding properties of a given sequence within a short duplex will mimic those in a long DNA fragment. The assumption of conformational equivalence in the present case is supported by the observation that the strong $[(OP)_2Cu^I]^+$ preference for the TAT triplet relative to flanking cytidines in sequences such as CCCTTATCCCC was clearly maintained in the undecamer duplex. Furthermore, the relative preferences of $[(OP)_2Cu^I]^+$ for PyPuPy triplets and the TAGT quartet found in restriction fragments were duplicated in oligonucleotide duplexes. Differences between the restriction fragment and TTATC duplex were observed, however, in the cleavages of the central adenosine relative to the 3′-flanking thymidine. These differences can be rationalized in terms of a slight shift of $[(OP)_2Cu^I]^+$ within the minor groove which rotates the copper away from the adenosine deoxyribose ring and toward the deoxyribose ring of the 3′-flanking thymidine (see also below). Small variations in conformation may be due to modest differences in ionic environment. On the whole, the oligonucleotide cleavage data suggest duplex conformations that are nearly identical with those for the same sequences in DNA restriction fragments.

The effects of single base pair transitions on $[(OP)_2Cu^I]^+$ cleavage preferences were examined by employing oligonucleotides that contain the highly preferred TAT or permutations of TAT, flanked by disfavored poly(C) tracts. Comparisons of the cleavages of oligonucleotides TCATC/G, TTACC/G, TTGTC, and TTATC clearly demonstrated that an A·T → G·C base pair transition diminished $[(OP)_2Cu^I]^+$ reactivity. Both the degree and causes of inhibition were dependent upon the position of the transition. A transition at position 1 (of the TAT triplet) was most detrimental, whereas a transition at position 2 had the least effect. These results predict the order of cleavage preferences for PyPuPy steps: TAT > TGT > TAC > CAT > TGC > CGT > CAC > CGC. This is in fact the order observed with restriction fragments (Veal & Rill, 1988), with the exception that TGC was slightly preferred over CAT, suggesting that a single transition at position 1 is more detrimental than transitions at both positions 2 and 3 of a PyPuPy triplet.

By contrast, only the A·T → I·C transition at position 3 diminished $[(OP)_2Cu^I]^+$ reactivity; duplexes with A·T → I·C transitions at positions 1 and 2 exhibited reactivities similar to TAT. The simplest interpretation of the latter result is that the guanine 2-amino group is primarily responsible for diminished $[(OP)_2Cu^I]^+$ cleavage at CAT and TGT triplets. The order of magnitude reduction in reactivity of the PyPuPy triplet in TCATC/G relative to TCATC/I dramatically demonstrates how a single DNA exocyclic substituent can markedly alter interactions of a simple ligand. Since cleavage was significantly diminished for both TTACC/G and TTACC/I relative to TTATC, inhibition of cleavage for G·C transitions at position 3 cannot be attributed to the guanine 2-amino group but instead may be the consequence of less obvious effects of sequence on local conformation.

In addition to direct effects of groove substituents, the local DNA conformation of TAT steps may be critical for preferential recognition by $[(OP)_2Cu^I]^+$. Substantial evidence indicates that poly[d(AT)] sequences can adopt an altered B-family conformation with helix twist angles significantly different from those of the canonical B form (Vorlickova & Kypr, 1985; Suzuki, 1986; Yoon et al., 1988). While several conformations have been proposed [e.g., alternating B and D DNA (Klug et al., 1979; Arnott et al., 1974)], they share in common an unusually narrow minor groove and large twist angles for TA steps. Whether TAT steps may adopt an altered conformation is unknown, but a locally altered conformation is one way of rationalizing the preference of $[(OP)_2Cu^I]^+$ for TAT over TAC steps. In particular, the occurrence of an unusually narrow minor groove at a TAT triplet, and not a TAC triplet, could explain the differences in cleavage preferences of these sequences if a narrow groove facilitates binding.

Although the sequence preferences of the $[(OP)_2Cu^I]^+$ complex have been determined in considerable detail, the actual mode of binding and the significance of third and fourth base effects remain unclear. Studies of DNA binding by the *N*-methylphenanthrolinium ion and substituted derivatives indicate that they intercalate (Gabbay et al., 1973), and intercalators in general prefer 5′-pyrimidine–purine-3′ steps to optimize base overlap. The initial work of Sigman's group supported intercalation for the $[(OP)_2Cu^I]^+$ complex (Marshall et al., 1981), whereas results of their recent use of $[(OP)_2Cu^I]^+$ to footprint *Eco*RI and netropsin binding sites (Kuwabara et al., 1986) are more consistent with groove binding.

Our data are consistent with either a groove binding or intercalation mechanism but can be rationalized most easily by a partial intercalation model as shown for dTA/dAT in Figure 7. Full intercalation is precluded by the tetrahedral coordination geometry of $[(OP)_2Cu^I]^+$. Partial intercalation allows energetically favorable stacking interactions between the central and one outer ring of the intercalated phenanthroline and the adenosines above and below. The hydroxyl radical generating copper is skewed toward one strand in a manner consistent with previous studies, showing that cleavages on strands opposing TAT are staggered in the 3′-direction and reduced in intensity. Moreover, it is apparent from the proposed model how a purine 2-amino group could inhibit binding at the PyPu step in a PyPuPy triplet. The amino group is sterically much larger than a proton and has a positive electrostatic potential that would repel the positive copper ion.

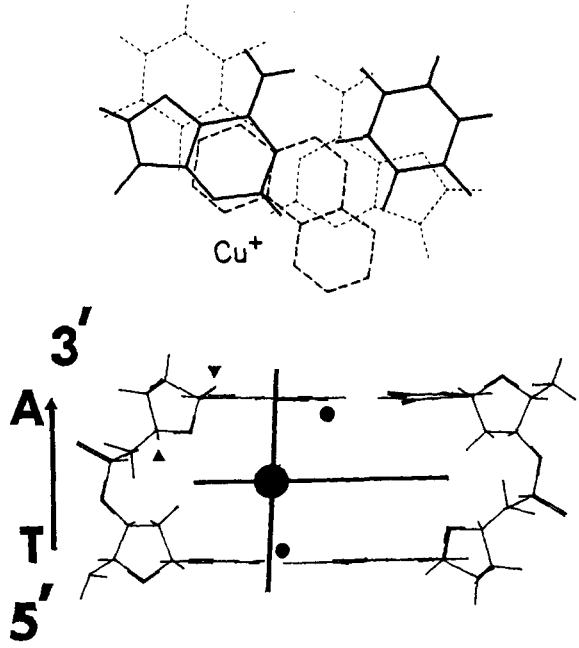

FIGURE 7: Partial intercalation model for binding of $[(OP)_2Cu^I]^+$ to the oligonucleotide duplex TTATC at the 5'-TpA-3' step (---, 5' T·A base pair; —, 3' T·A base pair). Partial intercalation allows for a placement of the copper ion, which is consistent with the observed cleavage frequencies for TTATC, and permits favorable stacking interactions between the phenanthroline ring system and the adenines above and below it. Top: Top view showing the proposed approximate position of the partially intercalated phenanthroline ring relative to the neighboring A·T base pairs. Bottom: Side view of the intercalation site facing the minor groove. The $[(OP)_2Cu^I]^+$ complex is shown schematically to emphasize the positions of the rings and the copper (large filled circle). The nonintercalated phenanthroline ring, represented here as a vertical line, would be skewed to the left and partially obscure the DNA backbone from this perspective. Positions of the C1' and C4' protons of the adenosine in a 5'-TpA-3' step are indicated by triangles. Approximate positions of adenine C2 protons are shown as small filled circles. A strong interaction is predicted between the nonintercalated phenanthroline ring and the guanine 2-amino group in a CpA step, and a lessor interaction is predicted for a TpG step. (The representation of an intercalation site shown in the bottom figure was kindly provided by W. David Wilson, Department of Chemistry, Georgia State University.)

Examination of models showed that steric exclusion should be greater for the sequence CAT than for TGT, and no steric effect was evident for TAC.

This model is also consistent with the biased distributions of specific products derived from oligonucleotide duplexes. According to Sigman and co-workers (Sigman, 1986; Kuwabara et al., 1986; Goyne & Sigman, 1987), attack of the hydroxyl radical at C4' yields 3'-phosphoglycolate, whereas attack at C1' produces the 3'-phosphomonoester and 3'-phospho-5-methylfuranone intermediate. An equivalent intrinsic reactivity of hydroxyl radicals toward the C1' and C4' protons is suggested by observations that ^{60}Co irradiation of a DNA solution yields equal amounts of 3'-phosphomonoester and 3'-phosphoglycolate products (Henner et al., 1982, 1983; Kuwabara et al., 1986). The band intensities corresponding to 3'-phosphomonoester and furanone products can be summed to represent the total reactivity at C1', which exceeded the reactivity at C4' at all positions in the PyPuPy triplet. The location of the copper shown in Figure 7 is consistent with the observed cleavage pattern for TTATC. The copper is most proximal to the C1' hydrogen of the adenosine deoxyribose, and the next closest hydrogen is C1' of the 3'-flanking thymidine. Partial intercalation places the copper ion deep within the minor groove. Attack at C1' is expected to predominate over C4' since the C1' proton points directly into the minor groove while C4' points away from the groove. The C4' hydrogen of the 3'-flanking thymidine is the third most proximal proton, although shielded somewhat by the second, nonintercalated phenanthroline. Cleavage of the TTATC, TTITC, and TTACC/I duplexes did yield more phosphoglycolate product (from C4') from the T7 (or C7) than from A6 (or I6) (Table II). In addition, the C1' and C4' hydrogens of C8, which were nearly equally reactive in TTATC, are approximately equidistant from the copper in this model. Finally, the reduced cleavage of the thymidine at position 5 relative to the thymidine at position 7 is reconciled in that T5 is both shielded and twisted away from the copper relative to T7.

The relative distances of the copper to different deoxyribose protons are markedly altered, in terms of this model, by slightly rotating the complex in the plane of the bases. Perhaps most interesting is a comparison of the individual nucleotide products at positions 6 and 7 of TTATC and TTGTC (Table II). The latter oligomer yielded relatively more phosphoglycolate (the C4' product) from the purine and less phosphoglycolate from the 3'-flanking thymidine. These results are expected from a simple rotation that places the copper nearer to the groove center, almost directly below the thymidine C1' and more distant from the guanosine C1'. Such movement may improve stacking interactions with the guanine or minimize effects of the guanine 2-amino group.

While a partial intercalation model is consistent with the observed cleavage pattern, including the product breakdown for individual bases, a reasonably acceptable groove binding model can also be constructed. Elucidation of the sequences preferred and disfavored by $[(OP)_2Cu^I]^+$ has permitted construction of an oligonucleotide duplex that should contain only one significant binding site. The cleavage data reported here are consistent with the existence of a single strong binding site in the TTATC oligomer. Strong binding to this site should be directly demonstrable and, if verified, allow determination of the binding mode by NMR methods.

ACKNOWLEDGMENTS

We thank Hank Henricks of the Department of Chemistry Biochemical Analysis and Synthesis Laboratory for technical assistance in the synthesis and purification of oligonucleotides and W. David Wilson (Department of Chemistry, Georgia State University) for providing graphics materials.

Registry No. $[(OP)_2Cu^I]^+$, 17378-82-4; CCCTTATCCCC·GGGGACAAGGG, 119367-33-8; CCCTTGTCCCC·GGGGACAAGGG, 119367-36-1; CCCTTACCCCC·GGGGITAAGGG, 119367-39-4; CCCTCATCCCC·GGGGATGAGGG, 119367-42-9; CCCTTTTCCCC·GGGGACAAGGG, 119367-44-1; CCCTTAGTCCC·GGGACTAAGGG, 119367-47-4; CCCTCATCCCC·GGGGATIAGGG, 119391-11-6; CCCTTACCCCC·GGGGGTAAGGG, 119367-50-9; TTATC, 119367-51-0; TTGTC, 119367-52-1; TTACC, 119367-53-2; TTITC, 119367-54-3; TTAGT, 119367-55-4; guanine, 73-40-5.

REFERENCES

Arnott, S., Chandrasekaran, R., Hukin, D., Campbell Smith, P. J., & Watts, L. (1974) *J. Mol. Biol. 88*, 523–533.
Barton, J. K. (1986) *Science 233*, 727–733.
Calladine, C. R. (1982) *J. Mol. Biol. 161*, 343–352.
Cartwright, I. A., & Elgin, S. (1982) *Nucleic Acids Res. 10*, 5835–5852.
Chen, C. H., & Sigman, D. S. (1986) *Proc. Natl. Acad. Sci. U.S.A. 83*, 7147–7151.
Chen, C. H., & Sigman, D. S. (1987) *Science 237*, 1197–1201.
Dickerson, R. E. (1983) *J. Mol. Biol. 166*, 419–441.

Dickerson, R. E., & Drew, H. (1981) *J. Mol. Biol. 149*, 761–786.
Drew, H., & Travers, A. (1984) *Cell 37*, 491–502.
Flick, J. T., Eissenberg, J. C., & Elgin, S. C. (1986) *J. Mol. Biol. 190*, 619–633.
Francois, J.-C., Saison-Behmoaras, T., Chassignol, M., Thuong, N. T., Sun, J.-S., & Helene, C. (1988) *Biochemistry 27*, 2272–2276.
Frederick, C. A., Grable, J., Melia, M., Samudzi, C., Jen-Jacobsen, L., Wang, B. C., Greene, P., Boyer, H. W., & Rosenberg, J. M. (1984) *Nature 309*, 327–331.
Gabbay, E. J., Scofield, R. E., & Baxter, C. S. (1973) *J. Am. Chem. Soc. 95*, 7850–7857.
Goyne, T., & Sigman, D. (1987) *J. Am. Chem. Soc. 109*, 2846–2848.
Henner, W. D., Grunberg, S. M., & Haseltine, W. A. (1982) *J. Biol. Chem. 257*, 11750–11754.
Henner, W. D., Rodriguez, L. D., Hecht, S. M., & Haseltine, W. A. (1983) *J. Biol. Chem. 258*, 711–713.
Jesse, B., Gargiulo, G., Razvi, F., & Worcel, A. (1982) *Nucleic Acids Res. 10*, 5823–5834.
Klug, A., Jack, A., Viswamitra, M. A., Kennard, O., Shakked, Z., & Steitz, T. A. (1979) *J. Mol. Biol. 131*, 669–680.
Kopka, M. L., Yoon, C., Goodsell, D., Pjura, P., & Dickerson, R. E. (1985) *Proc. Natl. Acad. Sci. U.S.A. 82*, 1376–1380.
Kuwabara, M., Yoon, C., Goyne, T., Thederhan, T., & Sigman, D. (1986) *Biochemistry 25*, 7401–7408.
Marshall, L. E., Graham, D. R., Reich, K. A., & Sigman, D. (1981) *Biochemistry 20*, 244–250.
Miller, K., & Pycior, J. (1979) *Biopolymers 18*, 2683–2719.
Sigman, D. (1986) *Acc. Chem. Res. 19*, 180–186.
Spassky, A., & Sigman, D. S. (1985) *Biochemistry 24*, 8050–8056.
Suggs, W., & Wagner, R. (1986) *Nucleic Acids Res. 14*, 3703–3715.
Suzuki, E., Pattabiraman, N., Zon, G., & James, T. (1986) *Biochemistry 25*, 6854–6865.
Tung, C. S., & Harvey, S. (1986) *J. Biol. Chem. 261*, 3700–3709.
Veal, J. M., & Rill, R. L. (1988) *Biochemistry 27*, 1822–1827.
Vorlickova, M., & Kypr, J. (1985) *J. Biomol. Struct. Dyn. 3*, 67–83.
Yoon, C., Prive, G., Goodsell, D., & Dickerson, R. (1988) *Proc. Natl. Acad. Sci. U.S.A. 85*, 6332–6336.

Comparison of the Fc Fragment from a Human IgG1 and Its CH2, pFc′, and tFc′ Subfragments. A Study Using Reductive Methylation and ^{13}C NMR†

Joyce E. Jentoft* and Richard Rayford
Department of Biochemistry, Case Western Reserve University, Cleveland, Ohio 44106
Received September 1, 1988; Revised Manuscript Received December 28, 1988

ABSTRACT: The Fc fragment of a human monoclonal IgG1 was compared with subfragments containing (a) the intact CH2 domain (CH2 fragment) or (b) the intact CH3 domain (pFc′ and tFc′ fragments). All fragments were reductively ^{13}C-methylated and their resulting dimethyllysyl resonances characterized in 0.1 M KCl as a function of pH by ^{13}C NMR spectroscopy. Seven resonances were characterized for the 18 lysine residues of the Fc fragment, eight for the 12 lysines of the CH2 fragment, and five each for the 9 lysines of the pFc′ and the 6 lysines of the tFc′ fragments, respectively. The multiplicity of resonances indicates that the lysine residues in each fragment exist in a variety of microenvironments and that the fragments are all highly structured. The correspondence between 6 of the 12 or 13 perturbed lysine residues in the Fc fragment and the smaller subfragments indicates that the conformation of the CH2 and CH3 domains is largely unchanged in the smaller fragments. However, in addition to three lysines at the CH2–CH3 domain interface, whose environments were known to be disrupted in the smaller fragments, three or four lysine residues have somewhat different properties in the Fc fragment and in the subfragments, indicating that some local perturbations are induced in the domain structure in the subfragments. Tentative partial assignments of dimethyllysyl resonances to lysine residues are suggested on the basis of comparisons of the properties of dimethyllysyl resonances in Fc and subfragments and on the interactions of lysyl residues in crystalline Fc [Diesenhofer, J. (1981) *Biochemistry 20*, 2361–2378].

Many of the biological functions associated with the IgG molecule are mediated through macromolecular interactions with sites in the Fc region, which contains the CH2 and CH3 constant domains. These interactions are preserved in proteolytic fragments containing either the Fc region or intact domains. The CH2 domain mediates catabolism of IgG (Dorrington & Painter, 1974) and is associated with complement fixation and antibody-dependent cytotoxicity (Yasmeen et al., 1976; Ellerson et al., 1972), while the CH3 domain has been shown to mediate the heterologous binding of human IgG to guinea pig peritoneal macrophages (Yasmeen et al., 1973), the binding to homologous macrophages (Okafor et al., 1975), and the release of histamine from mast cells (Minta & Painter, 1972).

Because of the biological importance of these immunoglobulin domains, we have embarked on detailed structure–function studies of the Fc fragment and single domain sub-

† This work was supported by grants-in-aid from the American Heart Association, Northeast Ohio Affiliate, by an NSF fellowship to R.R., and by Northeast Ohio Arthritis Center Grant AR 20618 from the National Institutes of Health.
* Author to whom correspondence should be addressed.

0006-2960/89/0428-3250$01.50/0